BL25SU
Soft X-ray Spectroscopy of Solid

1. Introduction

BL25SU is utilized for soft X-ray spectroscopic studies on electronic/magnetic states and surface structures of condensed matter. The beamline consists of two branch lines. The A-branch boasts high-energy-resolution X-rays suitable for electron spectroscopy experiments, whereas the B-branch is optimized for providing nano-focused beams with small angle divergence [1–3] and is mainly used for X-ray magnetic circular dichroism (XMCD) experiments.

The main topics in the beamline apparatuses in FY2022 are as follows: i) commencement of the operation of the spectroscopic low-energy electron microscope (SPELEEM), ii) relocation and introduction of the successor apparatus for the scanning nano-XMCD microscope, and iii) construction of the automatic real space scanning program for micro-soft X-ray angle-resolved photoemission spectroscopy (ARPES).

2. Status of Experimental Apparatuses

2-1. Spectroscopic low-energy electron microscope (SPELEEM) (A-branch first station)

The SPELEEM apparatus (LEEM III with energy analyzer, ELMITEC GmbH), which had been operated at BL17SU [4] and was moved to BL25SU in August FY2021 [Fig. 1(a)], started operation for users' experiments in the 2022B term. Prior to the operation, the measurement software used at BL17SU [Fig. 1(b)] was substantially modified in order to control the BL25SU optics. With this software, sequential measurements of different conditions, X-ray absorption spectroscopy (XAS), chemical mapping, XMCD, X-ray photoemission spectroscopy, and others, are available.

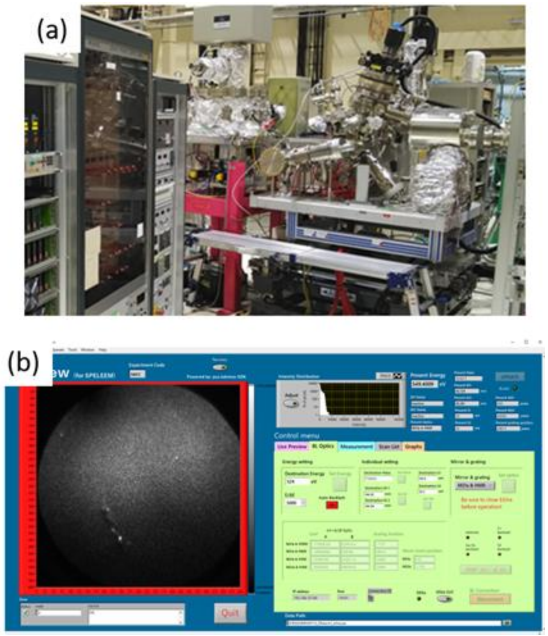

Fig. 1. a) SPELEEM apparatus installed at BL25SU. b) Measurement software (t-view) developed for BL25SU.

2-2. Retarding field analyzer (RFA) (A-branch second station)

Photoelectron holography can be used to study acyclic local structures with multiple chemical states [5]. This method requires wide-range photoelectron angular distribution patterns measured with sufficiently high energy resolution to resolve chemical shifts in the inner-core levels. A display-type RFA with a resolution ($E/\Delta E$) as high as 2000 is currently in operation to make such measurements [6]. Using this apparatus, the determination of dopant sites in BiS_2-based superconductors [7] and the elucidation of the arrangement of interfacial defects at the oxide layer of diamond semiconductors [8], for example, were achieved. In FY2022, a manipulator for sample cooling has been equipped to enable photoelectron holography experiments below 6 K.

2-3. Microbeam angle-resolved photoemission spectroscopy (ARPES) (A-branch third station)

The ability to select flatly cleaved areas (which are, in many cases, microscopic) from poorly cleaved sample surfaces is valuable for ARPES [9]. To enhance this capability, a micro-ARPES end-station equipped with a DA30 analyzer of Scienta Omicron and a micro-focusing mirror was developed [10, 11]. The typical focusing size is 0.4 μm (vertical) × 10 μm (horizontal). The beam spot size on the sample surface is as small as 10 μm even at a glancing angle of 5 degrees. This end-station has been open for public use since FY2018. In FY2022, an automatic real-space scanning program was constructed. This program is coded using LabVIEW software and allows the user to freely select a 1D, 2D, or 3D scan mode. Considering the spot size, the scanning step can be set to ~1 μm at minimum. Currently, we are building an analysis macro using Igor software.

2-4. Electromagnet-type XMCD spectroscopy (B-branch second station)

Electromagnet-type XMCD is a versatile XMCD apparatus that provides various experimental conditions. Its manipulator can attach one of three types of sample holders: for low temperature, for high temperature, and for measurements under electric force or current flow. The method of signal detection can also be selected from total electron yield (TEY), partial fluorescence yield (PFY), and transmission modes. A high-precision manipulator introduced in FY2020 allows measurements of microscopic areas. In FY 2022, to comply with the recent surge in the helium price, manipulator cooling using liquid nitrogen was tested (Fig. 2). As a result, although operation at the fully cooled temperature (77 K) was achievable, setting to specific temperatures was not successful owing to insufficient heater output. Further strategies are currently under consideration.

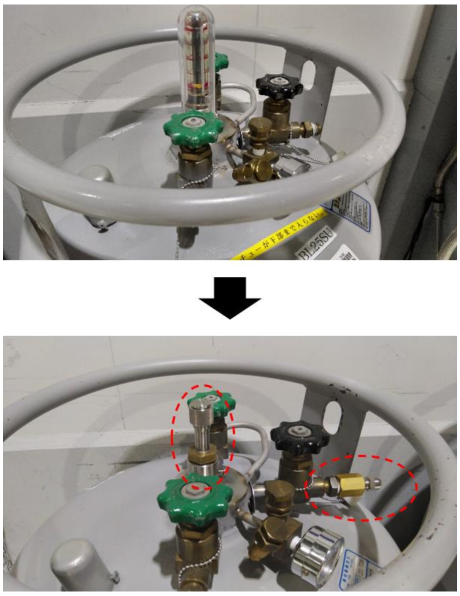

Fig. 2. Vessel adaptor compatible with a liquid helium transfer tube and a pressure regulation valve (red dotted circles) made for low-temperature XMCD measurements using liquid nitrogen.

2-5. Scanning soft X-ray microscope (nano-XMCD) (B-branch third station)

The scanning soft X-ray microscope developed with the support of the Elements Strategy Initiative Center for Magnetic Materials (ESICMM) funded by the Ministry of Education, Culture, Sports, Science and Technology (MEXT) of Japan [12, 13], which features nanoscale XMCD imaging under high magnetic fields up to 8 T, finished its operation in SPring-8 at the end of the 2022B term and is planned to be moved to another institution in FY2023. A successor apparatus with a similar design will be installed at the same station.

Ohkochi Takuo, Yamagami Kohei, and Nakamura Tetsuro

Spectroscopy Division, Center for Synchrotron Radiation Research, JASRI

References:

[1] Nakamura, T. et al. (2014). *SPring-8 INFORMATION* **19**, 102–105.

[2] Nakamura, T. et al. (2015). *SPring-8/SACLA Research Report* **3(1)**, 186–200.

[3] Senba, Y. et al. (2016). *AIP Conf. Proc.* **1741**, 030044.

[4] Guo F. Z. et al. (2007). *Rev. Sci. Instrum.* **78**, 066107.

[5] Tsutsui, K. et al. (2017). *Nano Lett.* **17**, 7533.

[6] Muro, T. et al. (2017). *Rev. Sci. Instrum.* **88**, 123106.

[7] Li, Y. et al. (2022). *J. Phys. Soc. Jpn.* **91**, 054602.

[8] Fujii, N. M. et al. (2023). *Nano Lett.* **23**, 1189–1194.

[9] Fujiwara, H. et al. (2015). *J. Synchrotron Rad.* **22**, 776.

[10] Senba, Y. et al. (2020). *J. Synchrotron Rad.* **27**, 1103.

[11] Muro, T. et al. (2021). *J. Synchrotron Rad.* **28**, 1631.

[12] Kotani, Y. et al. (2018). *J. Synchrotron Rad.* **25**, 1444–1449.

[13] Billington, D. et al. (2018). *Phys. Rev. Mater*. **2**, 104413.